ELSEVIER

Biophysical Chemistry 107 (2004) 151–164

Biophysical Chemistry

www.elsevier.com/locate/bpc

# Non-polar interactions between cholesterol and phospholipids: a molecular dynamics simulation study

Tomasz Róg, Marta Pasenkiewicz-Gierula*

*Department of Biophysics, Faculty of Biotechnology, Jagiellonian University, ul. Gronostajowa 7, Kraków 30-387, Poland*

Received 14 July 2003; received in revised form 4 September 2003; accepted 5 September 2003

**Abstract**

A 15-ns molecular dynamics simulation of the fully hydrated dimyristoylphosphatidylcholine-cholesterol (DMPC-Chol) bilayer containing ~22 mol% Chol was carried out. An 8-ns trajectory was analysed to investigate the effect of Chol on the chain packing in the bilayer core. While the packing of DMPC chains on the smooth α-face side of the Chol ring is similar to that in the pure DMPC bilayer, the packing on the rough β-face side is less regular and less tight. Two methyl groups located on the Chol β-face disturb the packing; in effect, van der Waals (vdW) interactions between Chol rings and DMPC chains are weaker than the ones between sole DMPC chains. VdW interactions between an alkyl chain of DMPC and an isooctyl tail of Chol are similarly strong as those between two DMPC chains.


*Keywords:* Phosphatidylcholine; Van der Waals interactions; Cholesterol α-face; Cholesterol β-face; Atom packing; Membrane condensation

## 1. Introduction

Cholesterol (Chol) is an important constituent of the animal cell membrane [1]. In prokaryots, only *Mycoplasma* contains cholesterol in its plasma membrane but this cholesterol is taken up from the host cell. Animal cells that are not able to synthesize cholesterol as well as *Mycoplasma* cells, to grow in the cell culture require Chol in the medium [2,3]. Chol analogues like 3α-methylcholesterol, lanosterol, and cholestanol may substitute for Chol, however, their concentration in the medium has to be much higher [3].

The Chol molecule consists of a planar tetracyclic ring system with the 3β-hydroxyl (Chol-OH) group and a short 8-carbon atom chain (isooctyl tail) attached to C17 (Fig. 1). In natural and model membranes [4] at temperatures above the main phase transition temperature for pure phospholipids, Chol effectively increases the order of saturated alkyl chains of phospholipids (ordering effect) [5,6] and the membrane surface density (condensing effect) [7,8]. These effects are essential for Chol to maintain proper fluidity [9], reduce passive permeability [10], and increase the mechanical strength [11] of the membrane. Chol

*Corresponding author. Tel.: +48-12-252-6518; fax: +48-12-252-6902.
*E-mail address:* mpg@mol.uj.edu.pl (M. Pasenkiewicz-Gierula).

0301-4622/04/$ - see front matter © 2003 Elsevier B.V. All rights reserved.
doi:10.1016/j.bpc.2003.09.002

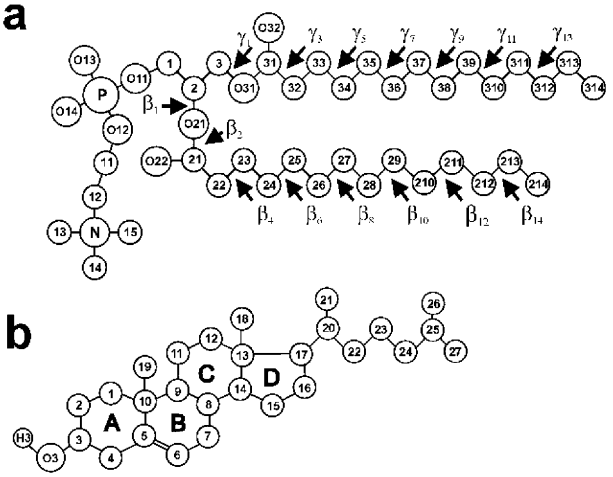


Fig. 1. Molecular structure with numbering of atoms of (a) DMPC, and (b) Chol (the chemical symbol for carbon atoms, C, is omitted). Torsion angles in the DMPC β- and γ-chain are indicated. The Chol rings are labelled A, B, C and D.

analogues, whose molecular structures often differ little from that of Chol, affect membrane ordering and condensation much less [12–21]. Thus, the molecular structure of Chol seems to be optimal for its biological membrane functions.

The Chol ring system is not symmetric about the ring plane and has a flat side with no substituents (α-face) and a rough side with two methyl substituents (β-face). The hydroxyl group is located on the β-face (cf. Fig. 2). Lanosterol, a precursor of Chol on its biosynthetic pathway, has three additional methyl substituents. Two of them are attached to C4, one on the α-and the other on the β-face. The third one is attached to C11 on the α-face. Conversion of lanosterol to Chol requires 19 enzymatic reactions and a large amount of energy. As other Chol analogues, lanosterol affects less than Chol membrane permeability [22], microviscosity [3,23], and condensation [24]. Also, it has a smaller than Chol effect on lateral diffusion of phosphatidylcholine (PC) molecules in the membrane [25]. Moreover, the phase diagram for a PC-lanosterol bilayer does not have a stable region of coexistence between the liquid-disordered and liquid-ordered phases [26,27]; the region is the most significant characteristics of the phase diagram for a PC-Chol bilayer [26–28]. An evolutionary process to remove both methyl groups from the lanosterol α-face might be thus regarded as optimisation of the sterol ring structure to make its interactions with the membrane lipids more effective [27,29–31].

The main goal of our molecular dynamics (MD) simulation studies of a dimyristoylphosphatidylcholine (DMPC) bilayer containing Chol has been to elucidate the relationship between the Chol structure and its effect on the bilayer made of fully saturated PC molecules. Our previous papers concentrated on the effect of Chol on the membrane/water interface [32,33] as well as the ordering [34] and condensing effects of Chol [35]. The study of the Chol ordering effect showed that the magnitude

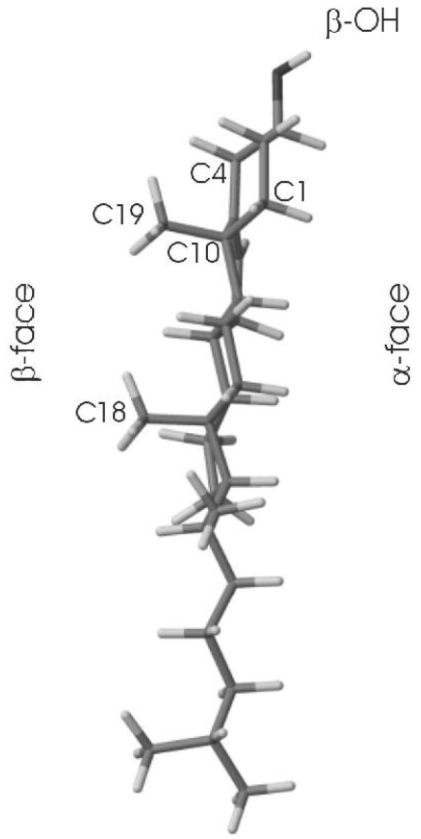


Fig. 2. Three-dimensional structure of Chol. The carbon and oxygen atoms are dark and the hydrogen atoms are grey. The smooth (α-face) and rough (β-face) faces of Chol are labeled.

of the Chol-induced ordering of a PC chain depends on the distance between the Chol molecule and the PC chain as well as on the side of the Chol molecule (α-or β-face) that the chain is in contact with; the smooth α-face promoting higher ordering than the rough β-face [34]. The study of the Chol condensing effect supported the hypothesis postulated by Hyslop et al. [36] that Chol induces an increase in both intra- and intermolecular van der Waals (vdW) interactions of the DMPC alkyl chains, while its vdW interactions with the chains are less favourable [35]. In that study, only an average effect of Chol on the PC chain packing was elucidated so a deeper understanding of PC–Chol interactions was still lacking.

This paper provides a more detailed picture of PC–Chol interactions that lead to the Chol condensing effect. The packing of PC chains around Chol is described in terms of the atom–atom radial distribution function (RDF). Analyses of RDFs indicate that the DMPC chain packing relative to the Chol α-face is similar to that in a pure DMPC bilayer, whereas relative to the Chol β-face is less tight due to the disturbing effect of the two methyl groups protruding from the Chol β-face. In effect, vdW interactions between Chol rings and DMPC chains are less strong than between sole DMPC chains. The analyses additionally demonstrate that the shape of RDF calculated relative to an atom in the Chol ring and tail is very sensitive to the atom's position and its chemical type.

## 2. Methods

### 2.1. Simulation systems

A DMPC-Chol bilayer membrane used in this study consisted of 56 DMPC, 16 Chol (approx. 22 mol% Chol), and 1622 water molecules. Details concerning the construction and MD simulation of this bilayer are described in Refs. [32,34]. In each leaflet, the Chol molecules were initially uniformly distributed and well separated from one another by DMPC molecules. The simulation was carried out for the total time of 15 ns. Fig. 1 shows the structure and numbering of atoms in DMPC and Chol molecules.

### 2.2. Simulation parameters

The DMPC-Chol bilayer was simulated using AMBER 4.0 [37]. For DMPC and Chol, optimised potentials for liquid simulations (OPLS) parameters [38] were used. The procedure for supplementing the original OPLS base with the missing parameters for DMPC was described in Ref. [39] and for Chol in Ref. [32]. For water, TIP3P parameters [40] were used. The united-atom approximation was applied to the CH, $CH_2$, and $CH_3$ groups of DMPC and Chol. All other groups, in particular the OH group of the water molecule and the hydroxyl group of Chol were treated with full atomic details. The atomic charges of the DMPC molecule were taken from Ref. [41] (a detailed explanation is given in Ref. [39]). The atomic charges of the Chol molecule are given in Ref. [32].

### 2.3. Simulation conditions

Three-dimensional periodic boundary conditions with the usual minimum image convention were used. The SHAKE algorithm [42] was used to preserve the bond length of the water molecule and the hydroxyl group of Chol, and the time step was set at 2 fs [43]. The remaining covalent bonds were free to vibrate. Our recent comparative simulations [44] indicated that for bilayers built of neutral lipids, a simulation that employs truncation of nonbonded interactions gives similar conformations and ordering of lipids to those obtained in a particle-mesh Ewald [45] simulation. Therefore, to reduce calculation time, the cutoff simulation with a cutoff distance of 12 Å was employed in this study. To further reduce calculation time, each DMPC molecule was divided into six residues (cf. [46]), and each Chol molecule was divided into three residues (cf. [32]). Each residue was chosen in such a way that the total electrostatic charge on the residue was close to zero and the integrity of its chemical groups was preserved. The list of nonbonded pairs was updated every 25 steps.

Simulation was carried out at a constant temperature of 310 K (37 °C), which is above the main phase transition temperature for a pure

DMPC bilayer (approx. 23 °C), and a constant pressure (1 atm). Temperatures of the solute and solvent were controlled independently. Both the temperature and pressure of the system were controlled by the Berendsen method [47]. The relaxation times for temperatures and pressure were set at 0.4 ps and 0.6 ps, respectively. Applied pressure was controlled anisotropically, where each direction was treated independently and the trace of the pressure tensor was kept constant (1 atm).

### 2.4. Data analysis

RDF describes the probability of finding a particle β at a distance between $r$ and $r+\mathrm{d}r$ away from a particle α in a simulation box of the volume $V$ containing $N$ particles:

$$\mathrm{RDF} = \frac{V}{N}\left\langle \frac{n(r)}{4\pi r^2\ \mathrm{d}r} \right\rangle \quad (1)$$

where $n(r)$ is the number of particles β in the spherical ring of a radius $r$ and width d$r$ around the particle α; $4\pi r^2\mathrm{d}r$ is the ring volume; $\langle\rangle$ denotes the time and ensemble average. In this paper, only carbon–carbon RDFs of all carbon atoms in the hydrophobic core of the membrane relative to PC chain atoms or selected atoms of the Chol ring and tail were calculated. Pairs of atoms belonging to the same molecule were omitted when calculating RDF.

A neighbour is a carbon atom of a DMPC alkyl chain or a Chol molecule that is located not further than 7 Å away from a chosen carbon atom in the bilayer core and belonging to a different molecule. The distance of 7 Å corresponds to the minimum in RDF calculated for DMPC chains both in DMPC and DMPC-Chol bilayers [35]. The position of the minimum in the carbon–carbon RDF does not change along the DMPC chain but, as it is shown below, depends on the position (and type) of the carbon atom in the Chol molecule. Nevertheless, in this paper the same definition of a neighbour applies to DMPC and Chol.

Due to the rotation of a Chol molecule and the surrounding DMPC chains as well as exchange of neighbouring and bulk DMPC molecules, the relative arrangement of the lipid molecules in the bilayer changes in time [34]. Observing the system with a time resolution of over 4 ns would provide an average picture of Chol–DMPC interactions. To find out individual contributions to the Chol–DMPC interactions, RDFs as well as numbers of neighbours were calculated every 1 ps, which is the time interval of the analysed trajectory. This way, it was possible to selectively analyse interactions between DMPC chains and certain atoms located on the Chol α- or β-face.

Results presented below were obtained from an 8-ns trajectory generated between 7 and 15 ns of the MD simulation. Reported average values are time and ensemble averages. Errors in the derived average values are standard error estimates obtained from the block averaging procedure.

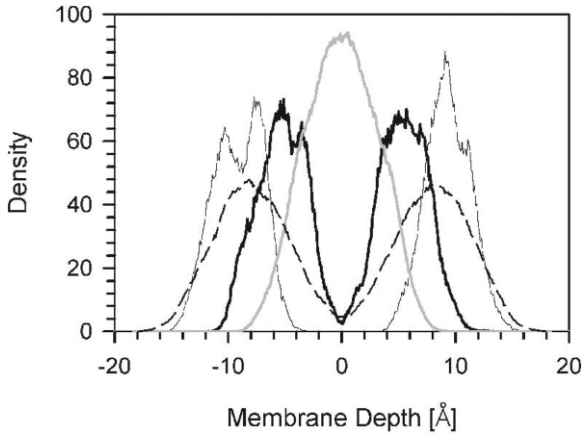


Fig. 3. Equilibrium number density profiles along the bilayer normal of the Chol ring (dashed line), and tail (grey line) atoms as well as the ring methyl groups C19 (thin line), and C18 (thick line). The centre of the horizontal axis (zero) is the middle of the bilayer core.

## 3. Results

### 3.1. Locations of atoms in the bilayer

Number density profiles of the Chol ring and tail atoms as well as the ring methyl groups (C19 and C18, cf. Fig. 2) along the bilayer normal are shown in Fig. 3. Positions of the methyl groups

Table 1
Numbers of neighbours (NS) and average distances from the bilayer centre of the Chol carbon atoms

| Chol atom | NS | $NS_{DMPC}$ | $NS_{Chol}$ | $NS_{\alpha}$ | $NS_{\beta}$ | Distance [Å] |
|---|---|---|---|---|---|---|
| C1 | 35.32 | 30.24 | 5.08 | 19.36 | 15.96 | 9.9 |
| C2 | 32.06 | 27.68 | 4.38 | 16.60 | 15.46 | 11.2 |
| C3 | 29.18 | 25.57 | 3.61 | 17.06 | 12.12 | 11.9 |
| C4 | 30.06 | 26.08 | 3.98 | 15.59 | 14.47 | 11.4 |
| C5 | 33.39 | 28.76 | 4.63 | 18.39 | 15.00 | 10.1 |
| C6 | 31.11 | 26.23 | 4.88 | 19.34 | 11.77 | 9.6 |
| C7 | 32.56 | 27.23 | 5.33 | 21.33 | 11.23 | 8.3 |
| C8 | 37.35 | 31.63 | 5.72 | 20.17 | 17.18 | 7.5 |
| C9 | 37.15 | 31.97 | 5.18 | 20.81 | 16.34 | 8.1 |
| C10 | 37.66 | 32.35 | 5.31 | 18.06 | 19.60 | 9.3 |
| C11 | 36.76 | 30.55 | 6.21 | 18.86 | 17.90 | 7.2 |
| C12 | 36.04 | 29.98 | 6.06 | 19.87 | 16.17 | 5.9 |
| C13 | 38.23 | 32.11 | 6.12 | 18.84 | 19.39 | 5.4 |
| C14 | 36.38 | 31.18 | 5.20 | 22.48 | 13.90 | 6.3 |
| C15 | 34.15 | 29.10 | 5.05 | 20.82 | 13.33 | 5.5 |
| C16 | 33.74 | 28.91 | 4.83 | 20.49 | 13.25 | 4.2 |
| C17 | 37.21 | 31.68 | 5.53 | 21.60 | 15.61 | 4.2 |
| C18 | 35.62 | 29.16 | 6.46 | 9.14 | 26.48 | 5.4 |
| C19 | 34.10 | 28.33 | 5.77 | 8.22 | 25.88 | 9.2 |
| Ring average | 34.64 | 29.41 | 5.23 | 18.27<br>19.39[a] | 16.37<br>15.22[a] | – |
| C20 | 37.55 | 31.34 | 6.21 | – | – | 3.1 |
| C21 | 36.63 | 29.71 | 6.92 | – | – | 2.9 |
| C22 | 35.68 | 30.00 | 5.68 | – | – | 1.9 |
| C23 | 36.76 | 31.37 | 5.39 | – | – | 0.9 |
| C24 | 39.94 | 34.23 | 5.71 | – | – | −0.1 |
| C25 | 43.03 | 36.71 | 6.32 | – | – | −0.9 |
| C26 | 42.50 | 36.94 | 5.66 | – | – | −1.5 |
| C27 | 42.78 | 35.54 | 7.24 | – | – | −1.4 |
| Tail average | 39.36 | 33.23 | 6.13 | – | – | – |
| Chol average | 36.03 (40.3[b]) | 30.54 | 5.49 | – | – | – |

Neighbours belonging to only DMPC ($NS_{DMPC}$) and only Chol ($NS_{Chol}$); neighbours of atoms located on the Chol α-face ($NS_{\alpha}$) and β-face ($NS_{\beta}$) belonging to either DMPC or Chol, are given. Errors in NS values are of the order of $\pm 0.02$ and in the distances are of the order of $\pm 0.1$ Å. For comparison, NS for a carbon of the DMPC chain is given in parentheses.

[a] Methyl groups C18 and C19 are not included.

[b] NS for a carbon atom of the DMPC chain.

along the normal cover the range of 12 Å in both membrane leaflets. Average distance of C19 from the bilayer centre is $9.2 \pm 0.1$ Å and that of C18 is $5.4 \pm 0.1$ Å. The location of C19 corresponds to average locations of DMPC atoms C26, C27, and C35 (9.9 Å, 8.8 Å, and 9.3 Å from the centre, respectively), and that of C18 corresponds to C210, C211, and C39 (6.0 Å, 5.0 Å, and 5.6 Å from the centre, respectively). Average distances of other Chol carbon atoms from the bilayer centre are given in Table 1. The sign '–' indicates that, on average, Chol tail atoms C24, C25, C26, and C27 are located in the opposite leaflet of the bilayer than the remaining Chol atoms.

Profiles along the DMPC β- and γ-chain of the probability that a given chain atom is a neighbour of the Chol ring methyl groups, C19 and C18, are shown in Fig. 4. As can be seen from the figure, atoms C24–C27 and C34–C36 are the most likely neighbours of C19, whereas the last eight atoms

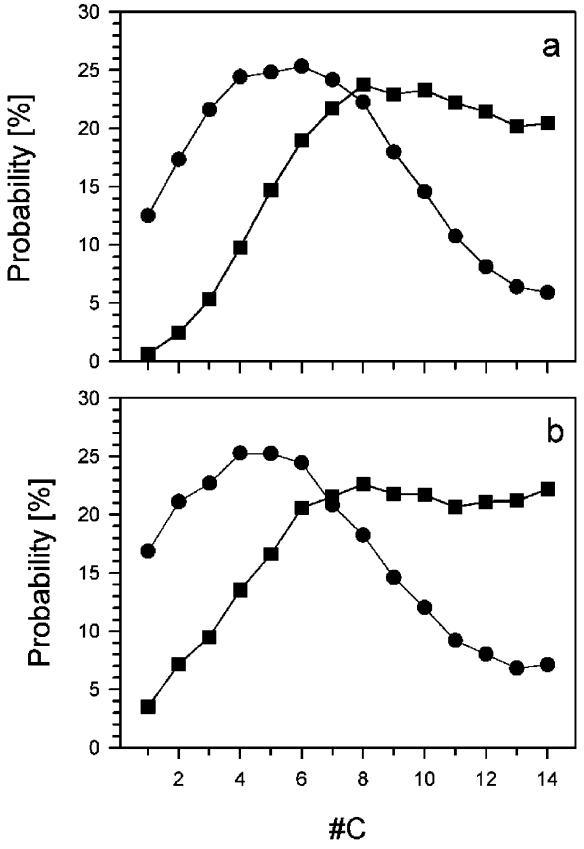


Fig. 4. Profiles of the probability that a carbon atom of the DMPC (a) β-chain and (b) γ-chain is a neighbour (cf. text) of the ring methyl group C18 (■) and C19 (●).

in both chains (C27–C214 and C37–C314) are the most likely neighbours of C18.

### 3.2. Atom packing in the bilayer core

RDFs of the carbon atoms in the hydrophobic core of the bilayer relative to a carbon atom of the DMPC alkyl chain, Chol ring, and Chol tail, averaged over all DMPC chain, Chol ring, and Chol tail atoms, respectively, are shown in Fig. 5a. RDF for a DMPC chain atom has two well resolved maxima, the first at the distance of 5 Å and the second at 9 Å, and a minimum at 7 Å. RDF for a Chol tail atom is similar, however, the first maximum and the minimum are flatter and shifted towards higher distances. In contrast, RDF for a Chol ring atom has no distinct extrema. Shapes of the RDFs indicate that packing of atoms around alkyl and isooctyl chains is more regular and dense than around the Chol ring. The average number of neighbours of a carbon atom in the DMPC alkyl chain is 40.3, in the Chol ring is 34.6, and in the Chol tail is 39.4 (Table 1). In each case, 80–85% of these neighbours are DMPC chain atoms (Table 1), the remaining 15–20% are Chol atoms, a fraction these atoms may belong to the opposite leaflet. Chol–Chol RDFs shown in

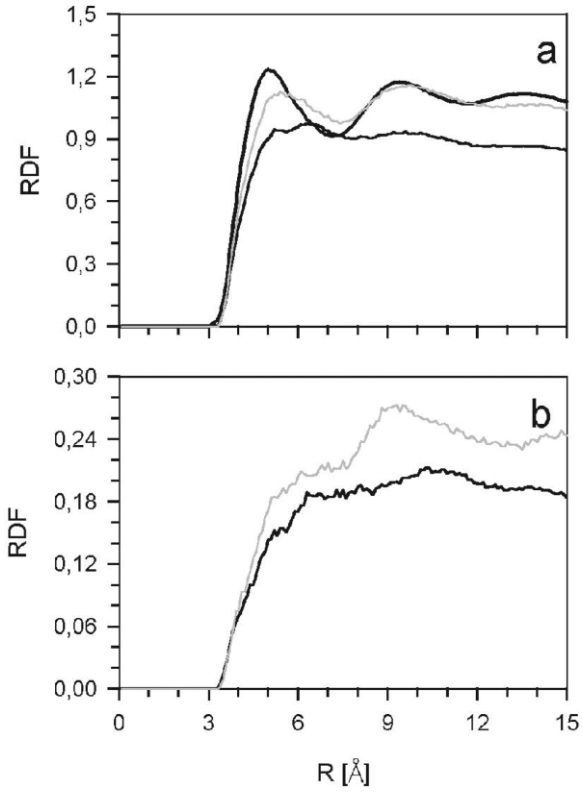


Fig. 5. Three-dimensional radial distribution functions (RDF) of (a) the carbon atoms in the bilayer core relative to a carbon atom of the DMPC alkyl chain (thick line), Chol ring (thin line), Chol isooctyl chain (grey line); (b) the Chol carbon atoms relative to a carbon atom of the Chol ring (solid line), and Chol isooctyl tail (grey line). In the calculations, pairs of atoms belonging to the same molecule were omitted.

Fig. 5b do not indicate any regular relative arrangement of Chol rings and tails in the bilayer.

### 3.3. Atom packing around selected Chol ring atoms

In order to find the cause for a less regular atom packing around the Chol ring, several RDFs of the atoms in the bilayer core relative to Chol carbon atoms of distinct chemical types were calculated (Figs. 6–10). The Chol atoms were classified into groups according to their types in the OPLS parameterisation: methyl groups (C18, C19), CT atoms (sp3 atoms with no hydrogen substituents C10, C13), CH atoms (sp3 atoms with one hydrogen substituent C3, C8, C9, C14, C17), $CH_2$ atoms (sp3 atoms with two hydrogen substituents C1, C2, C4, C7, C11, C12, C15, C16), and Sp2 atoms (C5, C6) (cf. Figs. 1 and 2).

To explain shapes of the RDFs shown in Figs. 6–10, each RDF was decomposed into two components; the first component (α component) was calculated for atoms located on the α-face side of the Chol ring and the second (β component) for atoms located on the β-face side. To establish whether a carbon atom C is located on the α-or β-face side, an angle between the C10–C19 bond (this bond is supposed to be perpendicular to the Chol ring faces, cf. Fig. 2) and the C10–C vector was calculated. For atoms located on the β-face, the angle is less or equal to 90° and for atoms located on the α-face, the angle is larger than 90°. When in calculations the C13–C18 bond was used instead of the C10–C19 bond the same results were obtained. Average numbers of neighbours of each Chol atom (NS), neighbours that were only DMPC ($NS_{DMPC}$) or Chol ($NS_{Chol}$) atoms as well as neighbours of atoms located on the Chol α-face ($NS_{\alpha}$) or β-face ($NS_{\beta}$), were also calculated (Table 1). As it was explained in Section 2, RDFs as well as numbers of neighbours were calculated every 1 ps and then averaged.

#### 3.3.1. CT atoms

RDFs calculated relative to CT atoms (C10, C13) and their α and β components are shown in Fig. 6. CT atoms, each connected with four carbon atoms, are buried inside the molecule. Therefore,

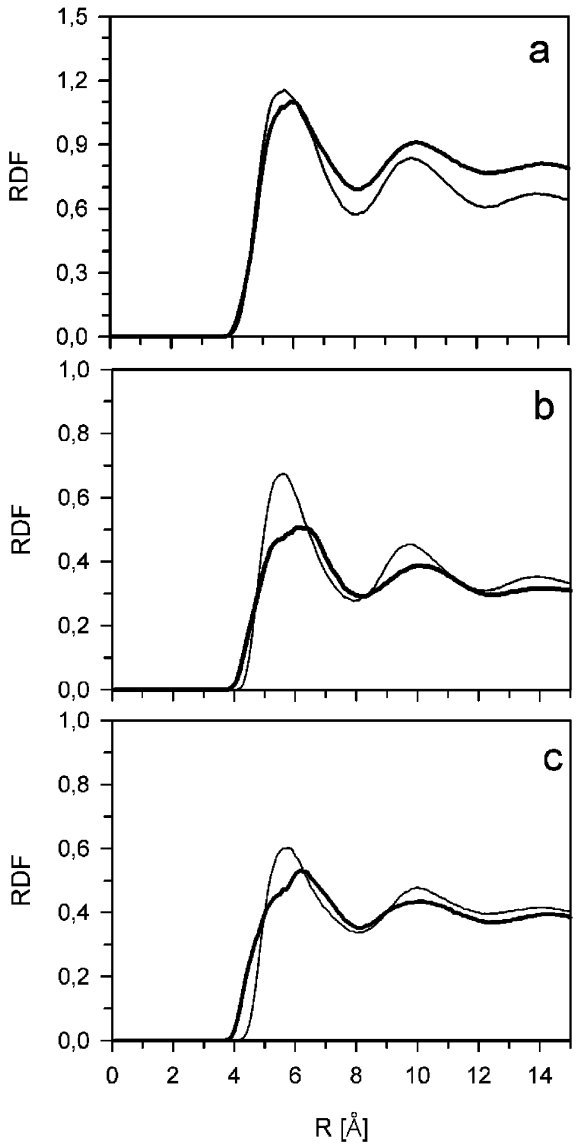


Fig. 6. Three-dimensional radial distribution functions (RDF) of the carbon atoms in the bilayer core relative to CT atoms. (a) C10 (thin line), and C13 (thick line); (b and c) α (thick line) and β (thin line) components of RDF for (b) C10, and (c) C13.

α and β components differ little from each other (Fig. 6b,c). Both components are shifted relative to RDF for a pure DMPC bilayer by less than 1.3 Å, i.e. less than one C–C bond length. A small

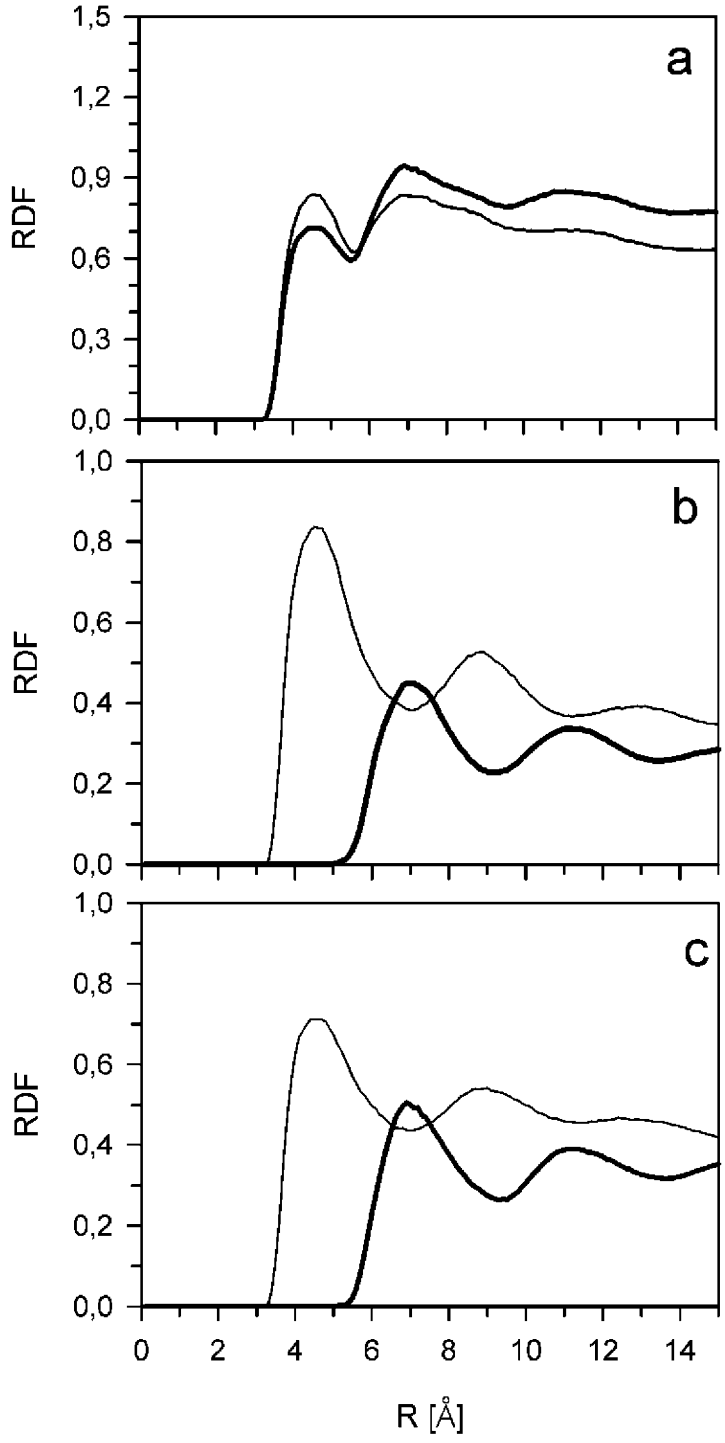


Fig. 7. Three-dimensional radial distribution functions (RDF) of the carbon atoms in the bilayer core relative to Chol methyl groups. (a) C19 (thin line), and C18 (thick line); (b and c) α (thick line) and β (thin line) components of RDF for (b) C19, and (c) C18.

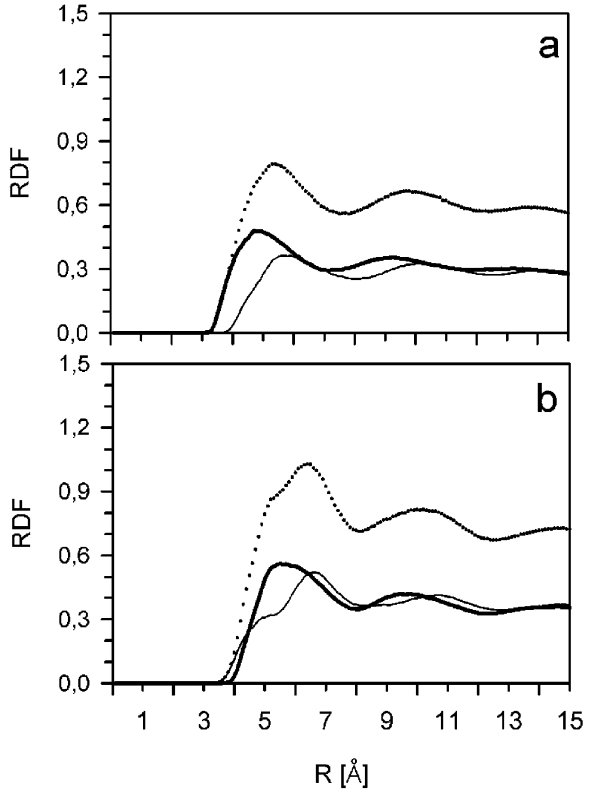


Fig. 8. Three-dimensional radial distribution functions (RDF) of the carbon atoms in the bilayer core relative to CH atoms (dotted line) as well as α (thick line) and β (thin line) components for (a) C3, and (b) C8.

relative shift of the β and α components is due to the two methyl groups that stick out of the β-face.

*3.3.2. Methyl groups*

RDFs calculated relative to methyl groups C19 and C18 are shown in Fig. 7a. Their α and β components have similar shapes, however, they are significantly shifted relative to each other (Fig. 7b,c). The β component almost overlaps with RDF for a pure DMPC bilayer; the α component is shifted by more than one C–C bond length, evidently because C19 and C18 stick out of the ring plane (cf. Fig. 2).

*3.3.3. CH atoms*

A CH atom of the Chol ring has a hydrogen substituent located either on the α-or β-face. With the help of Figs. 1 and 2 it becomes clear that in the first case, the atom is better exposed on the α-face (C3, C9, C14 and C17) and in the second case, it is better exposed on the β-face (C8). α components of RDFs calculated relative to C3 (Fig. 8a) as well as C9, C14 and C17 (data not shown) coincide with RDF for a pure DMPC bilayer, whereas β components are shifted by less than one C–C bond length (Fig. 8a). α and β components of RDF calculated relative to C8 (Fig. 8b) are less regular and shifted relative to RDF for a pure DMPC bilayer.

*3.3.4. $CH_2$ atoms*

$CH_2$ atoms of saturated six-carbon rings of Chol have the axial hydrogen substituent located either on the α-face (C1, C12) or β-face (C2, C4, C11). In the first case, the atoms are better exposed on the α-face and in the second, they are better exposed on the β-face. For $CH_2$ atoms that are located in the five-carbon ring (C15, C16) or next to the double bond (C7) none of the hydrogen substituents is on the α-or β-face; these atoms are equally exposed on both faces.

α components of RDFs for the $CH_2$ atoms, except for C4 (Fig. 9d), match RDF for a pure DMPC bilayer (Fig. 9a, b, c, e and f). β components are not shifted either, however, except for C7 (Fig. 9f), they show significant deviation from its shape (Fig. 9a, b, c, d and e). This deviation is most likely because atoms C1, C2, C11, C12 are located near the protruding methyl groups of the Chol ring (cf. Fig. 1). Similar deviations display β components of RDFs for C8 (Fig. 8b) and C14 (data not shown) that are located at ring junctions (cf. Fig. 1).

The location of the Chol hydroxyl group corresponds to the location of DMPC carbonyl groups [32]. So, the carbon atoms C1–C4 of the Chol ring A (cf. Fig. 1) are partially exposed to the bilayer interfacial region and their contact with the DMPC alkyl chains is less than that of the remaining Chol carbon atoms. This makes the extrema in RDFs for C1–C4 less resolved (Fig. 9a,c and d). Furthermore, the highly polar hydroxyl group of Chol additionally disturbs atom packing around them, especially around C4 (Fig. 9d).

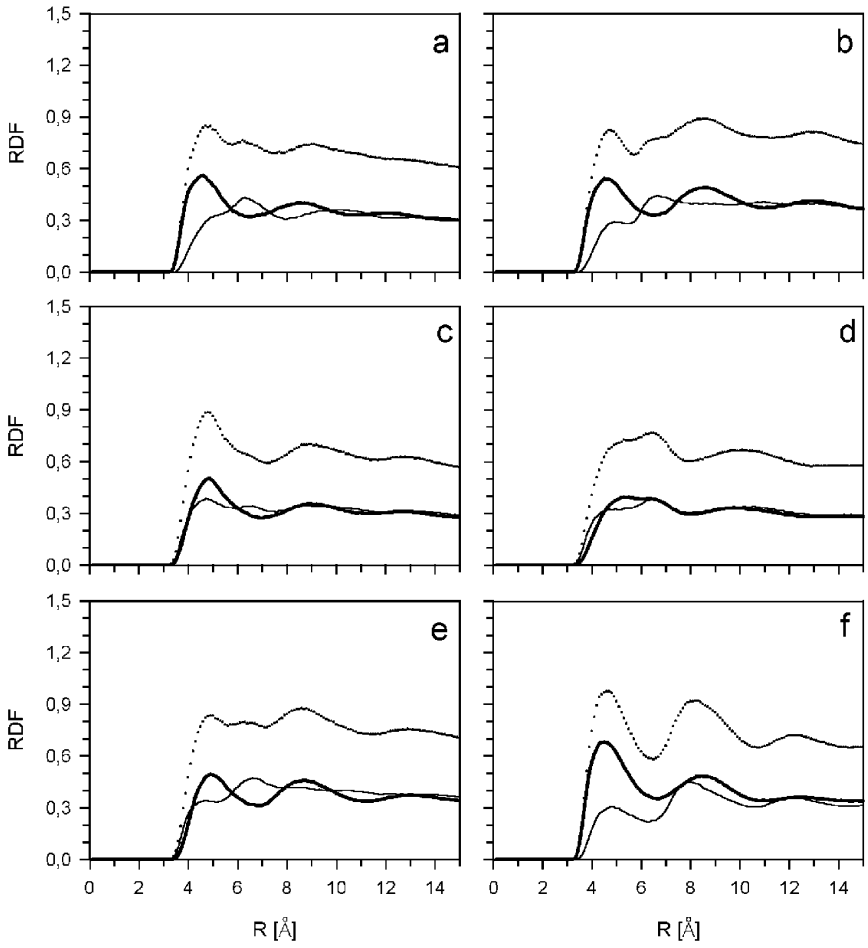


Fig. 9. Three-dimensional radial distribution functions (RDF) of the carbon atoms in the bilayer core relative to $CH_2$ atoms (dotted line) as well as their α (thick line) and β (thin line) components for (a) C1, (b) C12, (c) C2, (d) C4, (e) C11, and (f) C7.

*3.3.5. sp2 atoms*

There are two sp2 atoms in the Chol ring, C5 and C6. RDF for C6 overlaps with that for a pure DMPC bilayer, whereas RDF for C5 is shifted towards higher distances by approximately 0.5 Å (Fig. 10). This indicates that C6 is exposed on both sides of the ring, whereas C5 is buried inside the molecule (Fig. 10a). Indeed, both α and β components of RDF for C6 almost overlap (Fig. 10c) with RDF for a pure DMPC bilayer, whereas for C5 both components are shifted (Fig. 10b).

*3.4. Atom packing around Chol tail atoms*

RDFs of the carbon atoms in the bilayer core relative to selected Chol tail carbon atoms are shown in Fig. 11. RDFs for C27 and C26 (cf. Fig. 1) (Fig. 11a) as well as for C20, C24, and C25 (data not shown) are similar to RDF for a pure DMPC bilayer. RDF for the methyl group C21 (Fig. 11b) resembles RDFs for the ring methyl groups C18 and C19 (Fig. 6a), which are the superposition of α and β components (significantly shifted relative to each other) (Fig. 6b,c). Indeed, RDF for C21 can be decomposed into two components each calculated for the carbon atoms located on a different side of the plane perpendicular to the C20–C21 bond, in analogy to the α and β components (data not shown). The shape of RDFs for C22 and C23 indicates less favourable packing around these atoms (Fig. 11c).

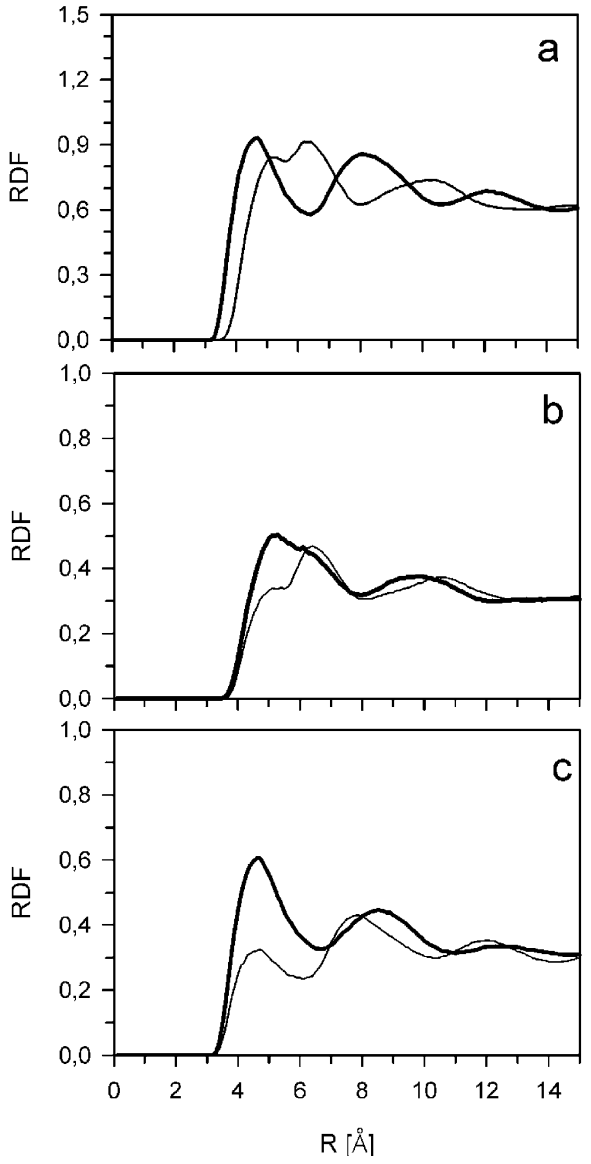


Fig. 10. Three-dimensional radial distribution functions (RDF) of the carbon atoms in the bilayer core relative to sp2 atoms. (a) C5 (thin line), and C6 (thick line); (b and c) α (thick line) and β (thin line) components of RDF for (b) C5, and (c) C6.

## 4. Discussion

In this paper, a detailed analysis of atom packing in the hydrophobic core of the DMPC bilayer containing 22 mol% Chol was performed. The tightness of packing is reflected in carbon–carbon RDF and can also be estimated by direct calculation of neighbours (cf. Section 2). The key result of the paper is that packing of carbon atoms on the Chol α-face side is tighter than on the β-face side. This conclusion can be drawn from direct comparison of shapes of α and β components of

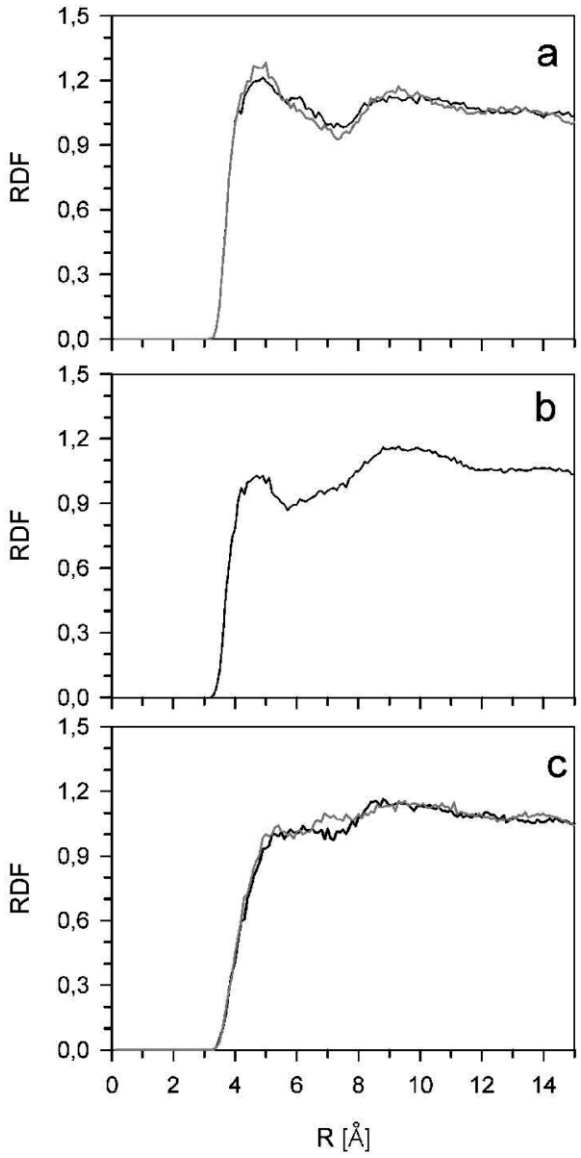


Fig. 11. Three-dimensional radial distribution functions (RDF) of the carbon atoms in the bilayer core relative to Chol isooctyl chain atoms. (a) C26 (black line), and C27 (grey line); (b) C21; (c) C22 (black line), and C23 (grey line).

RDFs for selected Chol ring atoms (e.g. Figs. 8 and 9 and Fig. 10). Furthermore, each atom located on the Chol α-face has, on average, ~19.5 neighbours and that located on the Chol β-face has ~15 neighbours. The former number constitutes a half of an average number of neighbours of each alkyl chain atom in a pure DMPC bilayer of ~40. So, packing of atoms around the Chol α-face is similar to that around a DMPC alkyl chain, whereas around the Chol β-face is less tight. This implies that vdW interactions of DMPC alkyl chains with the Chol α-face are stronger than with the β-face.

Konrad Bloch suggested [29] that removal of both methyl groups from the α-face of the sterol ring during evolution of the membrane sterols optimised vdW attraction between the sterol and phospholipid chains. This speculation was validated by higher microviscosity of a membrane containing Chol than its methylated precursors on the biosynthetic pathway [3,23] as well as by weaker condensing effect of lanosterol than Chol [24]. Our MD simulation studies support this hypothesis, as we see stronger vdW interactions between DMPC chains and demethylated smooth α-face than methylated rough β-face of the Chol ring. These results are in line with our previous results showing that the order of chains near the Chol α-face is grater than near the β-face [34]. Also, with numerous experimental as well as MD simulation data that indicate that the order of alkyl chains in bilayers containing lanosterol is less than that in bilayers containing cholesterol [12–15,24].

Experimental studies have shown that the isooctyl tail of Chol plays a significant role in interactions between Chol and phospholipids [21,48,49] as it facilitates PC-Chol vdW interactions [50]. Indeed, results obtained in our study indicate that vdW interactions between the tail and atoms that surrounds it are comparable to those between PC chains in a pure DMPC bilayer. The average number of neighbours of an isooctyl chain atom (39.4) is only slightly lower than that of a DMPC alkyl chain atom (40.3) but is much higher than that of a Chol ring atom (34.6) (Table 1). The strongest interactions are observed for the last four Chol tail atoms (C24, C25, C26 and C27).

At moderate Chol concentrations, DMPC and Chol are mixed well in a DMPC-Chol bilayer, as seen in the phase diagram of the binary mixtures of DMPC and Chol [51]. But in *cis*-unsaturated bilayers [52] it is segregated out. The lack of any regular relative arrangement of Chol molecules in the bilayer revealed the Chol–Chol RDF (Fig. 5b) as well as a relatively small number of neighbours of a Chol atom that originate from other Chol molecules (Table 1), indicate that indeed, Chol molecules are well separated from one another by DMPC molecules and have no tendency to segregate out into clusters.

The overall shapes of the RDFs for carbon atoms of hydrocarbon chains in the united atom approximation obtained from Monte Carlo simulations of liquid propane [53] and from MD simulations of liquid-crystalline bilayers made of pure phospholipids (DMPC, POPC) as well as a DMPC-Chol bilayer containing 22 mol% Chol [35,54], are similar. Thus, the locations of the two maxima at ~5 and ~9 Å, and the minimum at ~7 Å in the carbon–carbon RDF are basic characteristics of the bilayer core in the liquid-crystalline phase. Any deviation from this basic shape can be attributed to steric obstacles or additional interactions that disturb packing of atoms in the core. The position of the first maximum in the RDF of 5 Å is approximately equal to the sum of vdW radii of two carbon atoms in the united atom approximation, so the presence of the maximum indicates a close vdW contact between carbon atoms in the bilayer core.

The shape of RDF for a Chol ring atom as well as its α and β components is very sensitive to the atom's position in the ring, its distance from the bilayer surface, exposition on the ring α-or β-face, and finally, its chemical type. All ring atoms are carbon atoms of similar vdW parameters, e.g. vdW radii of the methyl and $CH_2$ group are 2.17 Å and 2.24 Å, respectively, thus, the observed sensitivity of atom packing on the atom type is surprising.

Our previous study showed [35] that atoms of the PC alkyl chain that are located deeper in the membrane core have more neighbours. A similar dependence was observed in this study for the Chol ring atoms, although not as clearly due to different chemical types and exposition on the α- or β-face of the ring atoms (see Table 1).

## Acknowledgments

T.R. holds a fellowship award from the Foundation for Polish Science in 2003. This work was supported by grant 6P04A03121 from the Committee for Scientific Research, Poland. All calculations were performed in the Academic Computational Centre Cyfronet, Kraków, Poland computational grant number KBN/SGI_ORGIN200/UJ/004/2000.

## References

[1] E. Sackmann, Structure and dynamics of membranes. From cells to vesicles, in: R. Lipowsky, E. Sackmann (Eds.), Biological Membranes, Architecture and Function, Elsevier, Amsterdam, 1995, pp. 1–63.

[2] M. Esfahani, L. Scerbo, T.M. Devlin, A requirement for cholesterol and its structural features for a human macrophage-like cell line, J. Cell Biochem. 25 (1984) 87–97.

[3] C.E. Dahl, J.S. Dahl, K. Bloch, Effect of alkyl-substituted precursors of cholesterol on artificial and natural membranes and on the viability of *Mycoplasma capricolum*, Biochemistry 19 (1980) 1462–1467.

[4] J.H. Davis, The description of membrane lipid conformation, order and dynamics by $^{2}$H-NMR, Biochim Biophys. Acta 737 (1983) 117–171.

[5] E. Oldfield, M. Meadows, D. Rice, R. Jacobs, Spectroscopic studies of specifically deuterium labeled membrane systems. Nuclear magnetic resonance investigation of the effects of cholesterol in model systems, Biochemistry 17 (1978) 2727–2740.

[6] T.P. Trouard, A.A. Nevzorov, T.M. Alam, C. Job, J. Zajicek, M.F. Brown, Influence of cholesterol on dynamics of dimyristoylphosphatidylcholine bilayers as studied by deuterium NMR relaxation, J. Chem. Phys. 110 (1999) 8802–8818.

[7] D. Marsh, I.O. Smith, Interacting spin labels as probes of molecular separation within phospholipid bilayers, Biochem. Biophys. Res. Comm. 49 (1972) 916–922.

[8] J.M. Smaby, M.M. Momsen, H.L. Brockman, R.E. Brown, Phosphatidylcholine acyl unsaturation modulates the decrease in the interfacial elasticity induced by cholesterol, Biophys. J. 73 (1997) 1492–1505.

[9] A. Kusumi, M. Tsuda, T. Akino, S. Ohnishi, Y. Terayama, Protein–phospholipid–cholesterol interaction in the photolysis of invertebrate rhodopsin, Biochemistry 22 (1983) 1165–1170.

[10] W.K. Subczynski, A. Wisniewska, J.-J. Yin, J.S. Hyde, A. Kusumi, Hydrophobic barriers of lipid bilayer membranes formed by reduction of water penetration by alkyl chain unsaturation and cholesterol, Biochemistry 33 (1994) 7670–7681.

[11] M. Bloom, E. Evans, O.G. Mouritsen, Physical properties of the fluid lipid-bilayer component of cell membranes: a perspective, Q. Rev. Biophys. 24 (1991) 293–397.

[12] J.A. Urbina, B. Moreno, W. Arnold, C.H. Taron, P. Orlean, E. Oldfield, A carbon-13 nuclear magnetic resonance spectroscopic study of inter-proton pair order parameters: a new approach to study order and dynamics in phospholipid membrane systems, Biophys. J. 75 (1998) 1372–1383.

[13] J.A. Urbina, S. Pekerar, H.B. Le, J. Patterson, B. Montez, E. Oldfield, Molecular order and dynamics of phosphatidylcholine bilayer membranes in the presence of cholesterol, ergosterol and lanosterol: a comparative study using $^{2}$H-, $^{13}$C- and $^{31}$P-NMR spectroscopy, Biochim. Biophys. Acta 1238 (1995) 163–176.

[14] P.L. Yeagle, Lanosterol and cholesterol have different effects on phospholipid acyl chain ordering, Biochim. Biophys. Acta 815 (1985) 33–36.

[15] C.E. Dahl, Effect of sterol structure on acyl chain ordering in phosphatidylcholine vesicles: a deuterium nuclear magnetic resonance and electron spin resonance study, Biochemistry 20 (1981) 7158–7161.

[16] M.A. Krajewski-Bertrand, A. Milon, Y. Nakatani, G. Ourisson, The interaction of various cholesterol'ancestors' with lipid membranes: a 2H-NMR study on oriented bilayers, Biochim. Biophys. Acta 1105 (1992) 213–220.

[17] E.J. Dufourc, E.J. Parish, S. Chitrakorn, I.C.P. Smith, Structural and dynamical details of cholesterol–lipid interaction as revealed by deuterium NMR, Biochemistry 23 (1984) 6062–6071.

[18] C. Faure, E.J. Dufourc, The thickness of cholesterol sulfate-containing membranes depends upon hydration, Biochim. Biophys. Acta 1330 (1997) 248–253.

[19] C. Faure, J.F. Tranchant, E.J. Dufourc, Comparative effects of cholesterol and cholesterol sulfate on hydration and ordering of dimyristoylphosphatidylcholine membranes, Biophys. J. 70 (1996) 1380–1390.

[20] A.M. Smondyrev, M.L. Berkowitz, Molecular dynamics simulation of dipalmitoylphosphatidylcholine membrane with cholesterol sulfate, Biophys. J. 78 (2000) 1672–1680.

[21] I.F. Craig, G.S. Boyd, K.E. Suckling, Optimum interaction of sterol side chains with phosphatidylcholine, Biochim. Biophys. Acta 508 (1978) 418–421.

[22] P.L. Yeagle, R.B. Martin, A.K. Lala, H.K. Lin, K. Bloch, Differential effects of cholesterol and lanosterol on artificial membranes, Proc. Natl. Acad. Sci. USA 74 (1977) 4924–4926.

[23] J.S. Dahl, C.E. Dahl, K. Bloch, Sterols in membranes: growth characteristics and membrane properties of *Mycoplasma capricolum* cultured on cholesterol and lanosterol, Biochemistry 19 (1980) 1467–1472.

[24] A.M. Smondyrev, M.L. Berkowitz, Molecular dynamics simulation of the structure of dimyristoylphosphatidyl-

choline bilayers with cholesterol, ergosterol, and lanosterol, Biophys. J. 80 (2001) 1649–1658.
[25] J.M. Polson, I. Vattulainen, H. Zhu, H. Zuckermann, Simulation study of lateral diffusion in lipid-sterol bilayer mixtures, Eur. Phys. J. E. 5 (2001) 485–497.
[26] M. Nielsen, J. Thewalt, L. Miao, J.H. Ipsen, M. Bloom, M.J. Zuckermann, et al., Sterol evolution and the physics of membranes, Europhys. Lett. 52 (2000) 368–374.
[27] L. Miao, M. Nielsen, J. Thewalt, J.H. Ipsen, M. Bloom, M.J. Zuckerman, et al., From lanosterol to cholesterol: structural evolution and differential effects on lipid bilayers, Biophys. J. 82 (2002) 1429–1444.
[28] M.R. Vist, J.H. Davis, Phase equilibria of cholesterol/dipalmitoylphosphatidylcholine mixtures: $^{2}$H nuclear magnetic resonance and differential scanning calorimetry, Biochemistry 29 (1990) 451–464.
[29] K. Bloch, Speculation on the evolution of sterol structure and function, CRC Crit. Rev. Biochem. 7 (1979) 1–5.
[30] D.E. Vance, H. Van den Bosch, Cholesterol in the year 2000, Biochim. Biophys. Acta 1529 (2000) 1–8.
[31] M. Bloom, O.G. Mouritsen, Structure and dynamics of membranes. From cells to vesicles, in: R. Lipowsky, E. Sackmann (Eds.), The Evolution of Membranes, Elsevier, Amsterdam, 1995, pp. 65–95.
[32] M. Pasenkiewicz-Gierula, T. Róg, K. Kitamura, A. Kusumi, Cholesterol effects on the phosphatidylcholine bilayer polar region: a molecular simulation study, Biophys. J. 78 (2000) 1376–1389.
[33] M. Pasenkiewicz-Gierula, K. Murzyn, T. Róg, C. Czaplewski, Molecular dynamics simulation studies of lipid bilayer systems, Acta Biochim. Pol. 47 (2000) 601–611.
[34] T. Róg, M. Pasenkiewicz-Gierula, Cholesterol effects on the phosphatidylcholine bilayer non-polar region: a molecular simulation study, Biophys. J. 81 (2001) 2190–2202.
[35] T. Róg, M. Pasenkiewicz-Gierula, Cholesterol effects on the phospholipid condensation and packing in the bilayer: a molecular simulation study, FEBS Lett. 502 (2001) 68–71.
[36] P.A. Hyslop, B. Morel, R.D. Sauerheber, Organization and interaction of cholesterol and phosphatidylcholine in model bilayer membranes, Biochemistry 29 (1990) 1025–1038.
[37] D.A. Pearlman, D.A. Case, J.C. Caldwell, G.L. Seibel, U.C. Chandra Singh, P.K. Weiner, et al., Amber 4.0, University of California, San Francisco, 1991.
[38] W.L. Jorgensen, J. Tirado-Rives, The OPLS potential functions for proteins. Energy minimizations for crystals of cyclic peptides and crambin, J. Am. Chem. Soc. 110 (1988) 1657–1666.
[39] M. Pasenkiewicz-Gierula, Y. Takaoka, H. Miyagawa, K. Kitamura, A. Kusumi, Charge pairing of headgroups in phosphatidylcholine membranes: a molecular dynamics simulation study, Biophys. J. 76 (1999) 1228–1240.
[40] W.L. Jorgensen, J. Chandrasekhar, J.D. Madura, R.W. Impey, M.L. Klein, Comparison of simple potential functions for simulating liquid water, J. Chem. Phys. 79 (1983) 926–935.
[41] P.S. Charifson, R.G. Hiskey, L.G. Pedersen, Construction and molecular modeling of phospholipid surfaces, J. Comp. Chem. 11 (1990) 1181–1186.
[42] J.P. Ryckaert, G. Ciccotti, H.J.C. Berendsen, Numerical integration of the cartesian equations of motion of a system with constraints: molecular dynamics of n-alkanes, J. Comp. Phys. 23 (1977) 327–341.
[43] E. Egberts, S-J. Marrink, H.J.C. Berendsen, Molecular dynamics simulation of a phospholipid membrane, Eur. Biophys. J. 22 (1994) 432–436.
[44] T. Róg, K. Murzyn, M. Pasenkiewicz-Gierula, Comparison of the Ewald summation and cutoff methods in molecular dynamics simulations of charged and uncharged lipid bilayers, Acta Biochim. Pol. In press.
[45] U. Essmann, L. Perera, M.L. Berkowitz, T. Darden, H. Lee, L.G. Pedersen, A smooth particle mesh Ewald method, J. Chem. Phys. 103 (1995) 8577–8593.
[46] M. Pasenkiewicz-Gierula, Y. Takaoka, H. Miyagawa, K. Kitamura, A. Kusumi, Hydrogen bonding of water to phosphatidylcholine in the membrane as studied by a molecular dynamics simulation: location, geometry and lipid–lipid bridging via hydrogen bonded water, J. Chem. Phys. 101 (1997) 3677–3691.
[47] H.J.C. Berendsen, J.P.M. Postma, W.F. vanGunsteren, A. DiNola, J.R. Haak, Molecular dynamics with coupling to an external bath, J. Chem. Phys. 81 (1984) 3684–3690.
[48] J.P. Slotte, M. Jungner, C. Vilcheze, R. Bittman, Effect of sterol side-chain structure on sterol–phosphatidylcholine interactions in monolayers and small unilamellar vesicles, Biochim. Biophys. Acta 1190 (1994) 435–443.
[49] R. Bittman, Has nature designed the cholesterol side chain for optimal interaction with phospholipid, Subcell. Biochem. 28 (1997) 145–171.
[50] P. Mattjus, R. Bittman, C. Vilcheze, J.P. Slotte, Lateral domain formation in cholesterol/phospholipid monolayers as affected by the sterol side chain conformation, Biochim. Biophys. Acta 1240 (1995) 237–247.
[51] D.J. Recktenwald, H.M. McConnell, Phase equilibria in binary mixtures of phosphatidylcholine and cholesterol, Biochemistry 20 (1981) 4505–4510.
[52] M. Pasenkiewicz-Gierula, W.K. Subczynski, A. Kusumi, Influence of phospholipid unsaturation on the cholesterol distribution in membranes, Biochimie 73 (1991) 1311–1316.
[53] W.L. Jorgensen, J.D. Madura, C.J. Swenson, Optimized intermolecular potential functions for liquid hydrocarbons, J. Am. Chem. Soc. 106 (1984) 6638–6646.
[54] T. Róg, M. Pasenkiewicz-Gierula, Effects of epicholesterol on the phosphatidylcholine bilayer: a molecular simulation study, Biophys. J. 84 (2003) 1818–1826.